Preparation, Crystallization Behavior, and Melting Characteristics of β-Nucleated Isotactic Polypropylene Blends with Polyamide 6

Zhugen Yang, Zishou Zhang, Youji Tao, Kancheng Mai

Key Laboratory of Polymeric Composites and Functional Materials (Ministry of Education), Materials Science Institute, School of Chemistry and Chemical Engineering, Sun Yat-Sen University, Guangzhou 510275, People's Republic of China

Received 4 April 2008; accepted 2 October 2008
DOI 10.1002/app.29362
Published online 11 December 2008 in Wiley InterScience (www.interscience.wiley.com).

ABSTRACT: β-Nucleated isotactic polypropylene (iPP) blends with polyamide 6 (PA6) were prepared with a novel and highly efficient nano-$CaCO_3$-supported β-nucleating agent. Maleic anhydride grafted polypropylene (PP-*g*-MA), glycidyl methacrylate grafted polypropylene (PP-*g*-GMA), maleic anhydride grafted poly(ethylene octene) (POE-*g*-MA), and maleic anhydride grafted poly(ethylene vinyl acetate) (EVA-*g*-MA) elastomers were added to the blends as compatibilizers. The nonisothermal crystallization behavior and melting characteristics of β-nucleated iPP and its blends were investigated with differential scanning calorimetry and wide-angle X-ray diffraction. The results indicated that the β-iPP content in the β-nucleated iPP blends depended not only on the preparation conditions but also on the compatibilizer type. A high β-iPP content (>95%) in the β-nucleated iPP/PA6 blends was obtained. The addition of PP-*g*-MA, POE-*g*-MA, and EVA-*g*-MA to the β-nucleated iPP/PA6 blends increased the content of β-iPP but decreased the crystallization temperature of iPP in the β-nucleated iPP/PA6 blends. However, the addition of PP-*g*-GMA decreased the content of β-iPP in the β-nucleated iPP/PA6 blends. © 2008 Wiley Periodicals, Inc. J Appl Polym Sci 112: 1–8, 2009

Key words: compatibilization; crystallization; melt; poly (propylene) (PP); polyamides

INTRODUCTION

Isotactic polypropylene (iPP) has complex polymorphism with several crystalline modifications, such as α, β, and γ modifications.[1,2] α-iPP is a very common commodity plastic that is of practical use in many areas, such as the home appliance, automotive, and construction industries, because of its good properties and low price. However, its relatively low service temperature and low toughness under severe conditions limit its usage. Compared to α-iPP, β-iPP has several advantages, especially its high impact strength[3,4] and good toughness at room temperature as well as high thermal deformation temperature. However, the yield strength and elastic modulus of β-iPP are lower than those of α-iPP. Moreover, β-iPP is not stable and may transform into α-iPP under some conditions.[5,6] Up to now, the addition of β-nucleating agents has been an effective method for the preparation of β-iPP.[1,8–11]

To improve the properties of β-iPP, the blending of β-iPP with other polymers will become an increasingly important method. Cao et al.[12] observed that the addition of a β-nucleating agent increased the toughness of iPP and iPP/poly(ethylene octene) blends but decreased their tensile strength. Guo et al.[13] studied the mechanical properties and crystallization behavior of polypropylene (PP) blends modified by a β-nucleating agent. The notched impact strength of a homopolymerized PP/randomly copolymerized PP/block-copolymerized PP blend was improved by 40% without a loss of tensile strength or flexural strength.

More attention has also been focused on the stability of β-iPP in its blends because β-iPP may easily transform into α-iPP on account of the effect of the second component. It has been observed that β-iPP blends can be prepared without any difficulty if they are compounded with something amorphous (e.g., an elastomer),[14–16] and the most important factor in the formation of a blend with β-iPP is the α-nucleation effect of the second component.[15,17,18] If the temperature of the crystallization peak (T_c^p) of the second component with an α-nucleating effect is lower than that of iPP, it has little effect on the formation of β-iPP. On the contrary, if T_c^p of the second component with an α-nucleating effect is higher than that of iPP, it suppresses the formation of β-iPP. For example, in β-nucleated iPP/poly(vinylidene fluoride) (PVDF) and iPP/polyamide 6 (PA6) blends,

Correspondence to: K. Mai (cesmkc@mail.sysu.edu.cn).
Contract grant sponsor: National Natural Science Foundation of China; contract grant number: 50873155.

β-iPP cannot form even in the presence of a highly effective β-nucleated agent because of the strong α-nucleating ability and higher T_c^p of PVDF and PA6. Menyhárd and Varga[19] reported that an iPP matrix consisting mainly of α-iPP was formed already with a low PA6 content in noncompatibilized β-nucleated iPP/PA6 blends. However, a β-iPP matrix predominantly developed in the presence of a maleic anhydride grafted polypropylene (PP-*g*-MA) compatibilizer. They suggested that the formation of an α-iPP matrix in the absence of a compatibilizer is related to the selective encapsulation of the β-nucleating agent in the polar PA6 phase. Compatibilizers, in addition to their traditional benefits, assist with the distribution of the β-nucleating agent between both phases of the blends and promote the formation of a matrix rich in β-iPP. Zhang et al.[20] studied the β-to-α transformation of iPP in compatibilized iPP/PA6 blends. The β-to-α transformation in β-nucleated iPP/PA6 blends compatibilized by PP-*g*-MA could be activated only at elevated tensile testing temperatures. This is related to the increase in the tensile elongation at break with the tensile testing temperature increasing. The presence of PA6 particles in the predominantly β-iPP matrix has no influence on the β-to-α transformation.

In this article, a highly efficient nano-$CaCO_3$-supported β-nucleating agent was used to obtain iPP/PA6 blends with a high β-iPP content. The β-nucleated iPP/PA6 blends were prepared under different preparation conditions. PP-*g*-MA, glycidyl methacrylate grafted polypropylene (PP-*g*-GMA), maleic anhydride grafted poly(ethylene octene) (POE-*g*-MA), and maleic anhydride grafted poly(ethylene vinyl acetate) (EVA-*g*-MA) elastomers were added to the blends as compatibilizers. The effects of the compounding conditions, the PA6 content, the type of compatibilizer, and the content of the compatibilizer on the nonisothermal crystallization, melting characteristics, and β-iPP content in the blends were investigated.

EXPERIMENTAL

Materials

iPP (H030SG) (Nag gum, India) was copolymer-grade and was supplied by Reliance Industries, Ltd. [India; melt flow rate = 3 g/10 min (230°C, 2.16 kg)]. PA6 (grade M2800) (Jiangmen, Guangdong, China) had a relative viscosity of 0.28 and was supplied by Guangdong Xinhui Media Nylon Co., Ltd. [melt flow rate = 11 g/10 min (230°C, 2.16 kg)]. PP-*g*-MA, EVA-*g*-MA, POE-*g*-MA, and PP-*g*-GMA were commercial products and were supplied by Guangzhou Lushan Chemical Materials Co., Ltd., and the grafted contents of maleic anhydride (MA) and glycidyl methacrylate (GMA) were 1.0 and 1.1 wt %, respectively. A commercial grade of active nano-$CaCO_3$ (Enping, Guangdong, China) with a particle diameter between 40 and 60 nm was obtained from Guangping Chemical Industry Limited Co. (China); it had been pretreated with fatty acid in its production process. Aliphatic dicarboxylic acid was supplied by Shanghai Hongsheng Industry Co., Ltd. (Shanghai, China); its purity was 98%.

Specimen preparation

Before the blending, all the materials were adequately dried in a vacuum oven at appropriate temperatures for 12 h. The nano-$CaCO_3$-supported β-nucleating agent was prepared from aliphatic dicarboxylic acid supported on the surface of nano-$CaCO_3$ (1/50 w/w) in our laboratory.[21] Compatibilized and noncompatibilized β-nucleated iPP/PA6 blends were prepared with an internal mixer (Karlsruhe, Germany) (Rheocord 300p, Haake, Germany) at different temperatures and 50 rpm. In the nucleated iPP, the nano-$CaCO_3$-supported β-nucleating agent content was 5 wt % of iPP.

The iPP/PA6 (80/20 wt/wt) blends were prepared under different compounding conditions. In case A, the nano-$CaCO_3$-supported β-nucleating agent was added to the iPP phase first at the temperature of 240°C, and then PA6 was added with mixing for 8 min. In case B, iPP was first mixed with the β-nucleating agent for 5 min at the temperature of 180°C and then mixed with PA6 for 8 min at 240°C. In case C, the β-nucleating agent was added to the PA6 phase first at the temperature of 240°C, and then iPP was added with mixing for 8 min. In case D, the iPP/PA6 blend was melted at the temperature of 240°C, and then the β-nucleating agent was added to the homogenized melt of the iPP/PA6 blend with mixing for 8 min. In case E, the iPP/PA6 blend was melted at the temperature of 240°C for 8 min, then the blend was cooled to 180°C, and the β-nucleating agent was added at this temperature with mixing for 5 min. β-Nucleated iPP blends with various PA6 contents and compatibilized β-nucleated iPP/PA6 blends were prepared in case E.

Differential scanning calorimetry (DSC)

DSC measurements were made on a PerkinElmer DSC-7 thermal system (PerkinElmer Cetus Instruments, Norwalk, CT) in a nitrogen atmosphere. Calibration was performed with pure indium at the heating rate of 10°C/min. A specimen of about 5 mg was weighed very accurately. It was heated to 260°C at 200°C/min, held there for 5 min, and then cooled to 100°C at a cooling rate of 10°C/min. This controlled cooling temperature prevented β–α

transformation so that the polymorphic composition of the sample could be determined accurately for the melting curves.[1,14] The sample was reheated to 260°C at a heating rate of 10°C/min for a study of the melting characteristics. The crystallization and melting parameters were recorded from the cooling and reheating scans.

The percentage of β-iPP (Φ_β) was obtained from the crystallinities of α-iPP and β-iPP according to ref. 22:

$$\Phi_\beta(\%) = \frac{X_\beta}{X_\alpha + X_\beta} \times 100 \quad (1)$$

$$X_i(\%) = \frac{\Delta H_i}{\Delta H_i^\theta} \times 100 \quad (2)$$

where X_α and X_β are the crystallinities of α-iPP and β-iPP, respectively [which can be calculated separately according to eq. (2)]; ΔH_i is the calibrated specific enthalpy of fusion of either α-iPP or β-iPP; and ΔH_i^θ is the standard enthalpy of fusion of α-iPP and β-iPP (178 and 170 J/g, respectively).[23] Because the DSC curves of some samples exhibited both α-iPP and β-iPP fusion peaks, the specific enthalpies of fusion for α-iPP and β-iPP were determined according to the following calibration method.[24] A vertical line was drawn through the minimum between the α-iPP and β-iPP fusion peaks, and the total enthalpy of fusion was divided into α-iPP (ΔH_α^*) and β-iPP (ΔH_β^*) parts. Because the less perfect α-iPP melted before the maximum point during heating and contributed to ΔH_α^*, the true value of the β-iPP enthalpy of fusion (ΔH_β) was approximated by the multiplication of ΔH_β^* by calibration factor A:

$$\Delta H_\beta = A \times \Delta H_\beta^* \quad (3)$$

$$A = \left[1 - \frac{h_2}{h_1}\right]^{0.6} \quad (4)$$

$$\Delta H_\alpha = \Delta H - \Delta H_\beta \quad (5)$$

where h_1 and h_2 are the heights from the base line to the β-iPP fusion peak and minimum point, respectively (Fig. 1).[25]

Wide-angle X-ray diffraction (WAXD)

The WAXD patterns of the specimens were recorded at room temperature with a Rigaku D/Max 2200 unit equipped with Ni-filtered Cu Kα radiation in the reflection mode with a wavelength of 0.154 nm. For direct comparison, the specimens were prepared on a PerkinElmer DSC-7 thermal system under the following conditions: they were heated to 260°C at 200°C/min, held there for 5 min, and then cooled to 40°C at a cooling rate of 10°C/min. The operating conditions of the X-ray source were a voltage of 40 kV and a current of 30 mA in the 2θ range of 5–40° with a step scanning rate of 2°/min.

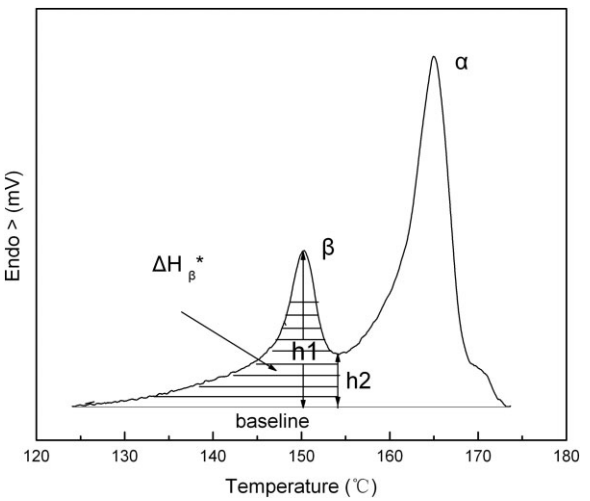

Figure 1 Schematic DSC melting curve of iPP showing the procedure for computing the β-crystal content.

RESULTS AND DISCUSSION

Effects of the compounding conditions

Figure 2 shows the crystallization and melting curves of β-nucleated iPP/PA6 blends prepared under different compounding conditions, and the relative parameters are listed in Table I. In Figure 2(a), the peaks appearing around 120 and 190°C can be attributed to the crystallization of iPP and PA6, respectively, and the β-nucleated iPP/PA6 blends exhibited the same crystallization behavior despite being prepared under different compounding conditions. Moreover, only a single crystallization peak of iPP can be observed in the curve, but the simultaneous crystallization of β-iPP and α-iPP took place during the cooling process. As shown in Table I, the compounding conditions did not have a distinct influence on T_c^p and the crystallization onset temperature (T_c^{on}) of iPP.

Multiple melting characteristics were observed [Fig. 2(b)] for β-nucleated iPP/PA6 blends prepared under different compounding conditions. Although double melting peaks appeared at about 220°C for β-nucleated iPP/PA6 blends (they were attributed to the melting of PA6), the compounding conditions had no pronounced influence on the melting characteristics of PA6. However, complex melting characteristics of iPP were observed in β-nucleated iPP/PA6 blends prepared under different compounding conditions. The peak near 160°C was related to the melting of α-iPP, and that appearing around 150°C

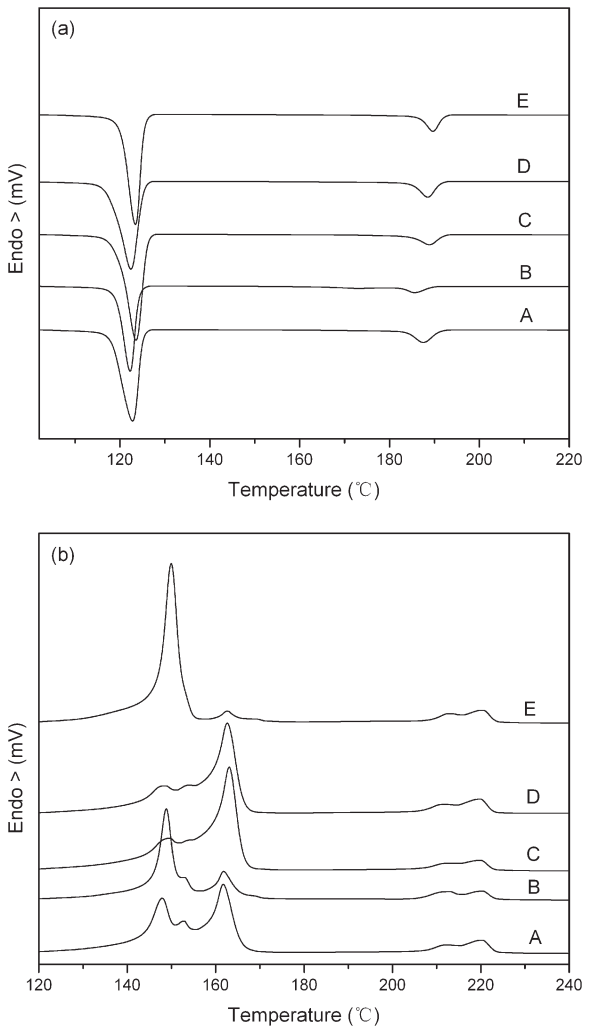

Figure 2 (a) Crystallization and (b) melting curves of iPP/PA6 blends prepared by different methods.

was attributed to the melting of β-iPP. Moreover, the intensity of the melting peak of β-iPP in the β-nucleated iPP/PA6 blend prepared in case E was the most intensive, and Φ_β reached 96.3%. In case E, iPP and PA6 were first melted at the temperature of 240°C, and then the nano-$CaCO_3$-supported β-nucleating agent was added to the blend as it was cooled to 180°C. In this case, the β-nucleating agent was mainly distributed into the iPP phase because the PA6 had crystallized but the iPP phase was still in a molten state. Therefore, the β-nucleating agent played a heterogeneous nucleating role in iPP crystallization, and the high β-iPP content was obtained. In case B, iPP was first mixed with the β-nucleating agent at the temperature of 180°C, and then the prepared β-iPP was homogenized with PA6 at 240°C. Φ_β decreased to 70.9% and was lower than that in case E. In other β-nucleated iPP/PA6 blends prepared at the temperature of 240°C, the addition of PA6 decreased the β-iPP content significantly. It has been suggested that the β-nucleating agent might disperse into the PA6 phase and/or interface between PA6 and iPP at the high temperature of 240°C because of the interaction of polar groups.[19] As a result, the efficient component of the β-nucleating agent would decrease in the iPP phase. On other hand, the interaction between the polar groups of the β-nucleating agent and PA6 may result in changes in its chemical structure and a reduction in the nucleation ability of the β-nucleating agent. According to ref. 22, the order of Φ_β is case E > case B > case A > case C > case D (Table I), and this indicates that it is quite dependent on the preparation conditions.

The WAXD spectra of β-nucleated iPP/PA6 blends prepared under different compounding conditions are shown in Figure 3. The diffraction peaks at 2θ values of 14.3, 16.8, and 18.6° correspond to the (110), (040), and (130) planes of α-iPP, and the one at 2θ = 16.1° corresponds to the (300) plane of the β-iPP.[26,27] The intensity of the diffraction peak at β (300) in case E was the strongest. The relative β-iPP content (K_β) was calculated according to the equation suggested by Turner Jones et al.:[28]

$$K_\beta = \frac{I_{\beta 1}}{I_{\beta 1} + I_{\alpha 1} + I_{\alpha 2} + I_{\alpha 3}} \tag{6}$$

where $I_{\beta 1}$, $I_{\alpha 1}$, $I_{\alpha 2}$, and $I_{\alpha 3}$ are the diffraction intensities of the β (300), α (110), α (040), and α (130) planes, respectively. According to eq. (6), K_β in each

TABLE I
DSC Data for the iPP Component in the iPP/PA6 Blends Prepared with Different Methods

Case	T_c^p (°C)	T_c^{on} (°C)	ΔH_c (J/g)	T_m^p (°C)		T_m^{on} (°C)		ΔH_m (J/g)		Φ_β (%)	K_β
				β	α	β	α	β	α		
A	122.8	125.1	81.7	147.9	161.7	143.1	157.5	41.3	31.6	41.9	0.409
B	122.3	124.2	85.6	148.8	161.8	146.1	159.5	54.1	15.6	70.9	0.728
C	123.6	126.0	84.6	149.6	161.1	141.7	158.8	31.6	40.4	18.3	0.268
D	122.4	125.2	82.3	150.9	162.6	141.3	158.3	31.1	43.6	15.6	0.209
E	122.2	125.4	87.9	150.2	162.7	146.9	160.3	78.0	2.5	96.3	0.981

The enthalpy has been corrected by the weight fraction. Φ_β and K_β have been calculated according to DSC and WAXD, respectively. ΔH_c = enthalpy of crystallization; ΔH_m = enthalpy of fusion; T_m^{on} = onset temperature of melting; T_m^p = temperature of melting peak.

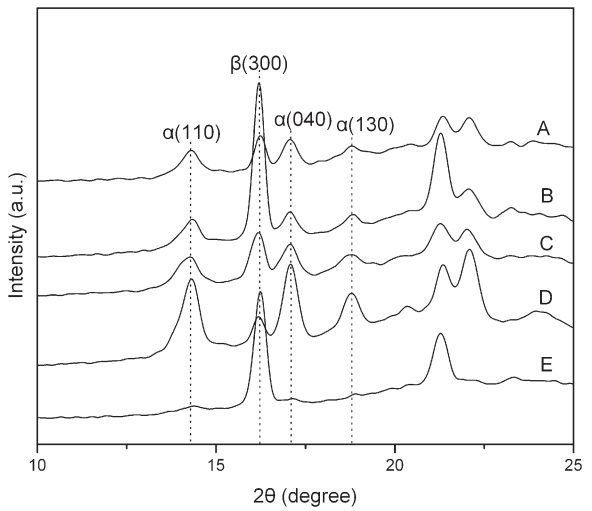

Figure 3 X-ray spectra of iPP/PA6 blends prepared by different methods.

case (A, B, C, D, and E) is listed in Table I (0.409, 0.728, 0.268, 0.209, and 0.981), and K_β of other blends is listed in Table II. It can be concluded that the results obtained from WAXD were similar to those from DSC.

Effect of the PA6 content

The crystallization and melting curves of β-nucleated iPP/PA6 blends prepared in case E are presented in Figure 4, and the relative data are listed in Table II. The results show that the content of PA6 had no influence on the crystallization behavior of iPP in the blends. As shown in Figure 4(a), T_c^p of iPP in the blends was influenced slightly by the PA6 content, but T_c^p of PA6 shifted to the high temperature with increasing PA6 content. Figure 4(b) illustrates that the melting characteristics of iPP were dependent on the PA6 content, and the intensity of the melting peak for β-iPP was very strong and higher than that of α-iPP in each blend. However, the single melting peak of β-iPP changed into double melting peaks and the intensity of the higher melting peak became much stronger with increasing PA6 content. Φ_β in each blend was very high, more than 95% (Table II), and this indicated that the addition of PA6 had no distinct influence on the β-iPP content in the blends.

Menyhárd and coworkers[18,19] observed that an iPP matrix consisting mainly of α-iPP was formed already at a low PA6 content in noncompatibilized β-nucleated iPP blends. They suggested that the addition of PA6 suppressed the formation of β-iPP because of PA6 as an α-nucleating agent and the selective encapsulation of the nucleating agent in the polar PA6 phase. In our study, what was interesting was that Φ_β could reach as high as 95% even though the PA6 content was 40 wt % in β-iPP/PA6 blends. It can be suggested that the β-iPP content in β-iPP/PA6 blends is quite dependent on the compounding conditions of the blends. When the β-nucleating agent was added to the blend at the temperature of 180°C, it was difficult for the β-nucleating agent to diffuse into the PA6 phase because the PA6 had been crystallized at the moment but the iPP phase was still in a molten state. Therefore, an iPP matrix consisting mainly of β-iPP was formed already at a high PA6 content.

Figure 5 shows the WAXD spectra of β-nucleated iPP/PA6 blends with various contents of PA6. There was only an intensive peak appearing at $2\theta = 16.1°$ with respect to the (300) plane of β-iPP when the PA6 content was low. However, a peak appeared at $2\theta = 14.1°$ corresponding to the (110) plane of α-iPP, and its intensity became stronger with increasing PA6 content. Besides, K_β slightly decreased with increasing PA6 content (Table II).

TABLE II
DSC Data for the iPP and PA6 Components in Noncompatibilized and Compatibilized iPP/PA6 Blends

iPP/PA6/ compatibilizer		T_c^p (°C)		ΔH_c (J/g)		T_m^p (°C)			ΔH_m (J/g)				
		PP	PA6	PP	PA6	β	α	PA6	β	α	PA6	Φ_β (%)	K_β
No compatibilizer	100/0/0	122.3	—	79.3	—	149.9	163.0	—	85.2	1.9	—	97.9	0.992
	90/10/0	121.7	186.4	80.8	51.0	150.0	162.2	219.2	86.0	2.1	53.0	97.7	0.985
	80/20/0	122.2	188.0	87.9	55.0	150.2	162.7	219.8	78.0	2.5	57.5	96.3	0.981
	70/30/0	122.3	188.1	88.4	61.7	148.6	161.1	219.5	85.9	4.0	64.0	95.9	0.963
	60/40/0	122.3	188.8	92.5	67.8	148.5	161.1	219.3	87.3	5.2	70.0	95.1	0.950
PP-*g*-GMA	80/20/5	122.6	186.3	87.0	37.3	149.8	162.7	219.2	51.6	17.0	49.6	71.2	0.723
EVA-*g*-MA	80/20/5	118.3	—	90.9	—	147.9	161.1	219.4	67.6	2.1	49.4	97.2	0.982
POE-*g*-MA	80/20/5	119.2	—	93.2	—	148.7	161.7	219.3	72.6	1.1	51.5	98.6	0.984
PP-*g*-MA	80/20/5	119.5	—	90.5	—	148.3	161.1	219.1	73.0	1.8	50.9	97.7	0.983
PP-*g*-MA	80/20/3	120.1	186.0	85.2	3.6	148.3	161.1	218.8	70.8	2.1	60.0	97.2	0.968
PP-*g*-MA	80/20/1	120.6	186.3	87.5	33.0	148.8	161.1	218.8	76.1	1.6	55.6	97.0	0.964

The enthalpy has been corrected by the weight fraction. ΔH_c = enthalpy of crystallization; ΔH_m = enthalpy of fusion; T_m^p = temperature of melting peak.

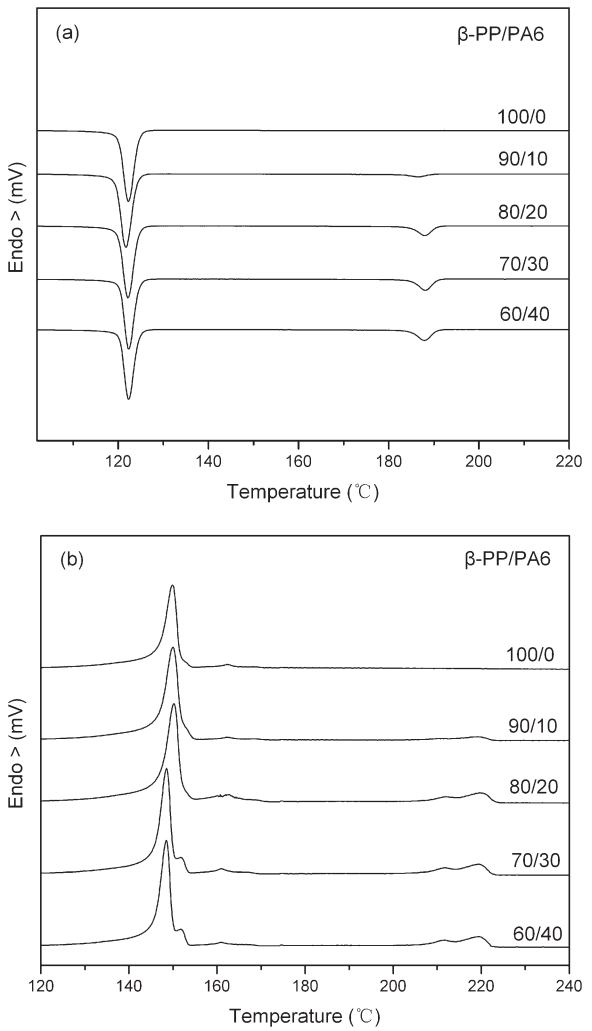

Figure 4 (a) Crystallization and (b) melting curves of iPP/PA6 blends with various contents of PA6 prepared in case E.

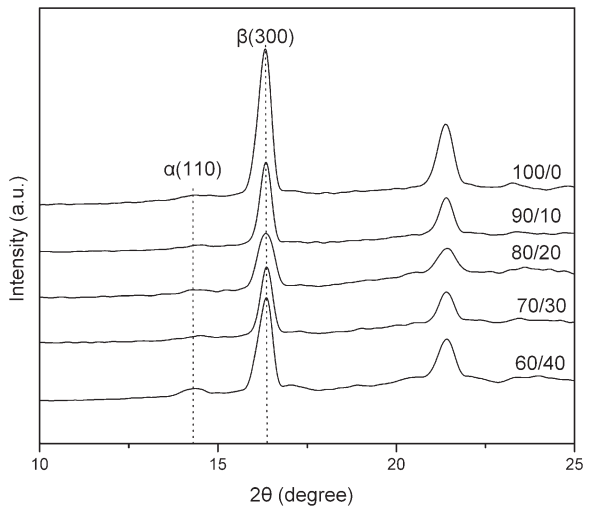

Figure 5 X-ray spectra of iPP/PA6 blends with various contents of PA6 prepared in case E.

Effects of the compatibilizers

Figure 6 presents the crystallization and melting curves of compatibilized β-nucleated iPP/PA6 (80/20) blends prepared in case E, and the relative data are listed in Table II. The addition of the compatibilizer had an obvious effect on the crystallization behavior of iPP and PA6 in the blends. The PA6 crystallization peak in the blends compatibilized with PP-*g*-MA, EVA-*g*-MA, and POE-*g*-MA is absent, but a tiny one can still be observed in its blends compatibilized with PP-*g*-GMA. This can be attributed to the fact that the addition of MA-grafted compatibilizers increased the homogeneity of the PA6 phase dispersion in the iPP matrix with a reduction in the size of the domains due to the compatibilization of the compatibilizers. The PP-*g*-PA6 copolymer formed at the interface, and this reduced the crystallizability of PA6.[29] However, the same functions of GMA-grafted compatibilizers were

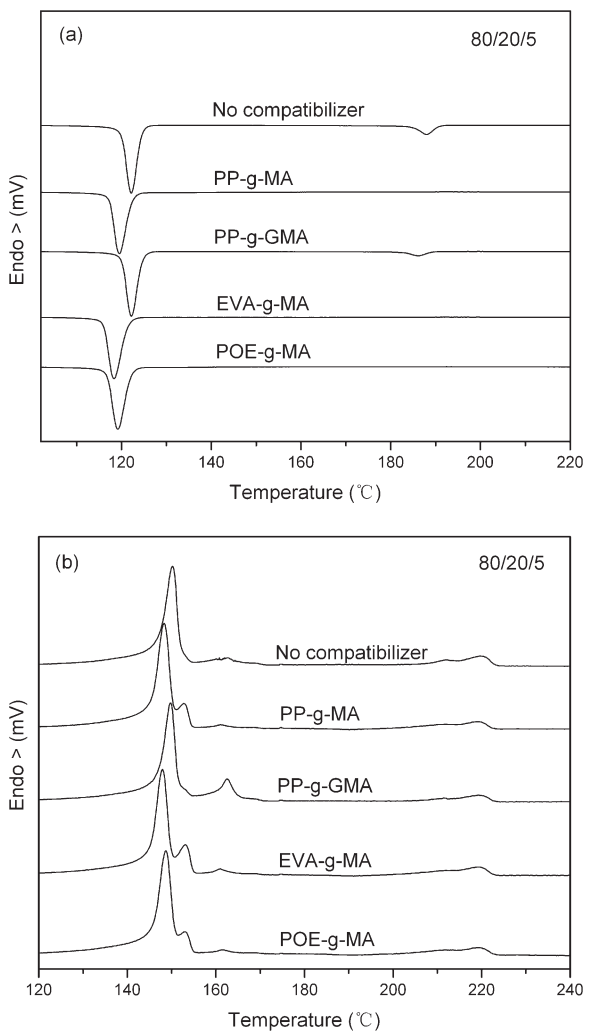

Figure 6 (a) Crystallization and (b) melting curves of iPP/PA6 blends modified with various kinds of compatibilizers (5 phr) prepared in case E.

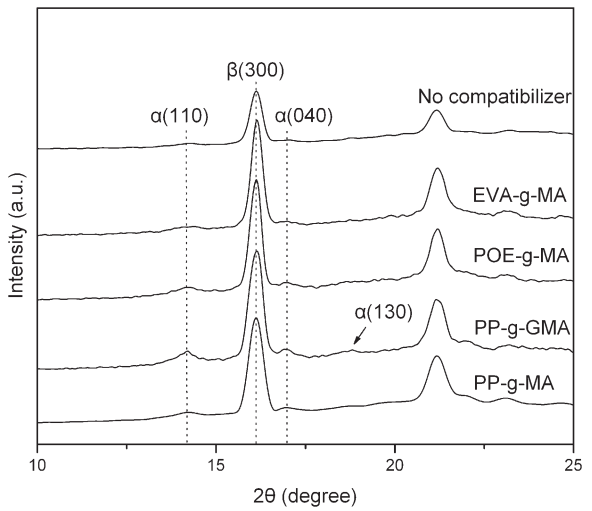

Figure 7 X-ray spectra of 80/20 iPP/PA6 blends with various kinds of compatibilizers (5 phr) prepared in case E.

weaker than those of MA-grafted ones because of weaker compatibilization. This can be attributed to the fact that the chemical reaction of the GMA-grafted compatibilizer with PA6 was weaker than that of the MA-grafted compatibilizer with PA6; besides, the polarity of the GMA-grafted compatibilizer was weaker than that of the MA-grafted one, so the compatibilization effect of PP-*g*-GMA on the blend was weaker than that of the MA-grafted ones.[30] Moreover, the addition of a compatibilizer also significantly influenced the crystallization behavior of iPP, and T_c^p of iPP in its blends compatibilized with PP-*g*-MA, EVA-*g*-MA, and POE-*g*-MA shifted to a low temperature. For example, T_c^p of iPP decreased from 122.2°C in a noncompatibilized blend to 118.3°C in a β-nucleated iPP/PA6 blend compatibilized with EVA-*g*-MA. However, the addition of PP-*g*-GMA had little influence on T_c^p of iPP in its blends because of the weaker compatibilization.

As shown in Figure 6(b) and Table II, the melting characteristics and the β-iPP content in the compatibilized β-nucleated iPP/PA6 blends depended on the compatibilizer type. Double melting peaks of β-iPP were observed, and the β-iPP content increased for β-nucleated iPP/PA6 blends compatibilized with PP-*g*-MA, POE-*g*-MA, and EVA-*g*-MA. For example, Φ_β in the blend compatibilized with POE-*g*-MA increased from 96.3 to 98.6%. This indicated that the compatibilizer with MA group resulted in the easy dispersion of the β-nucleating agent in the iPP phase and was beneficial for the formation of a matrix rich in β-iPP. Menyhárd et al.[31] also observed that MA-grafted iPP with a low MA content crystallized in the β form in the presence of β-nucleating agents. However, the addition of PP-*g*-GMA decreased the β-iPP content of iPP (71.2%) in the compatibilized β-nucleated iPP/PA6 blend, and this may be related to the interaction between the GMA group and the nucleating agent, which resulted in its chemical structure changing and the β-nucleating ability decreasing.

Figure 7 presents X-ray diffraction patterns of compatibilized β-nucleated iPP/PA6 blends; the peak at $2\theta = 16.1°$ with respect to β-iPP was very intensive in the compatibilized blends. However, a weak peak could be seen at $2\theta = 18.6°$ that belonged to the (130) plane in the blends compatibilized with PP-*g*-GMA, and this indicated that α-iPP was formed in the β-nucleated iPP/PA6/PP-*g*-GMA blend.

Effect of the PP-*g*-MA content

Figure 8 illustrates the crystallization and melting curves of β-nucleated iPP/PA6 blends compatibilized with various contents of PP-*g*-MA, and the relative data are also listed in Table II. T_c^p of iPP in the

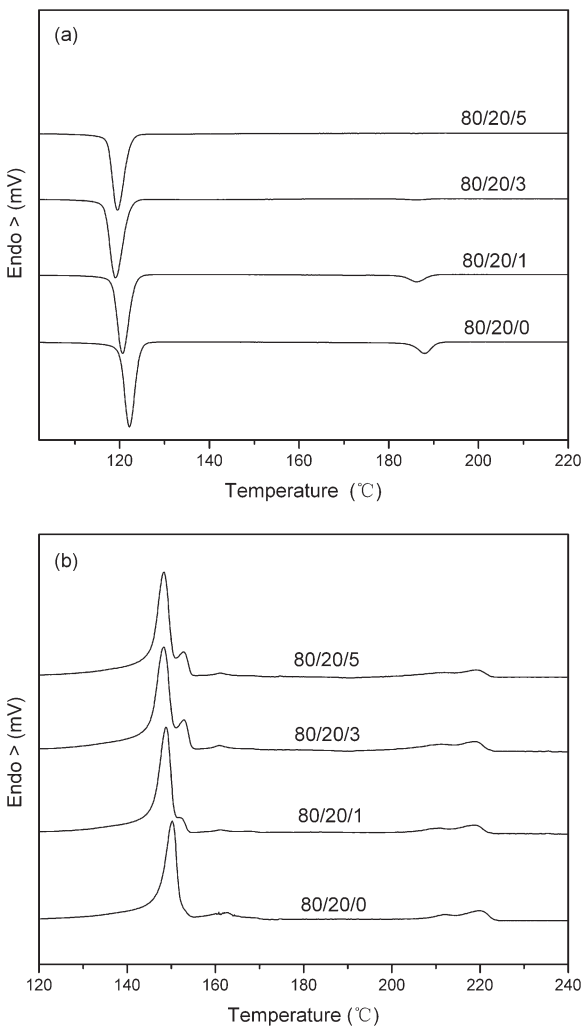

Figure 8 (a) Crystallization and (b) melting curves of 80/20 β-iPP/PA6 blends compatibilized with various contents of PP-*g*-MA prepared in case E.

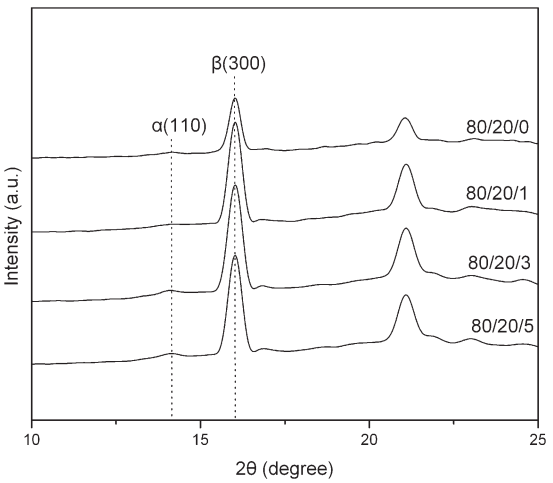

Figure 9 X-ray diffraction patterns of β-iPP/PA6 blends compatibilized with various contents of PP-*g*-MA prepared in case E.

compatibilized β-nucleated iPP/PA6 blends gradually decreased, and the crystallization peak of PA6 disappeared with increasing PP-*g*-MA content. This can be attributed to an increase in the compatibilization of PP-*g*-MA with its increasing content and to the promotion of the dispersion of PA6 into the iPP phase, which resulted in weakening of the crystalline ability of the PA6.[29,32] Although a tiny melting peak of α-iPP around 160°C was observed in the noncompatibilized β-nucleated iPP/PA6 blends, it became unobvious for the compatibilized β-nucleated iPP/PA6 blend. The double melting peaks of β-iPP can also be observed for the compatibilized blend in Figure 8(b), and the intensity of the melting peak at a high temperature became more and more obvious with increasing PP-*g*-MA content. However, Φ_β in each blend compatibilized with various contents of PP-*g*-MA was higher than 97% (Table II), and this indicated that the PP-*g*-MA content had little influence on the β-iPP content. In addition, the WAXD spectra of the blends (Fig. 9) also show that the peaks at $2\theta = 16.1°$, with respect to the (300) plane of β-iPP, are all very intensive, indicating that iPP crystallized predominantly in the β form.

CONCLUSIONS

On the basis of our results, the content of β-iPP in the β-nucleated iPP/PA6 blends depended on the compounding conditions. A high content of β-iPP could be obtained if the nucleating agent was added to the blends when the PA6 had been crystallized but the iPP phase was still in a molten state; as a result, the β-nucleating agent was mainly distributed in the iPP phase and produced heterogeneous nucleation in iPP crystallization. Moreover, in this case, the PA6 content had little influence on the β-iPP content. PP-*g*-MA, POE-*g*-MA, and EVA-*g*-MA reduced T_c^p of iPP and increased the β-iPP content in the β-nucleated iPP/PA6 blends, and this can be attributed to the fact that the compatibilizer improved the dispersion of PA6 in the iPP phase, resulting in a decrease in the crystalline ability and α-nucleating ability of PA6.

References

1. Varga, J. J Macromol Sci Phys 2002, 41, 1121.
2. Grein, C. Adv Polym Sci 2005, 188, 43.
3. Tjong, S. C.; Shen, J. S.; Li, R. K. Y. Scr Metall Mater 1995, 33, 503.
4. Karger Kocsis, J.; Varga, J.; Ehrenstein, G. W. J Appl Polym Sci 1997, 64, 2059.
5. Kotek, J.; Raab, M.; Baldrian, J.; Grellmann, W. J. J Appl Polym Sci 2002, 85, 1174.
6. Chen, H. B.; Karger-Kocsis, J.; Wu, J. S.; Varga, J. Polymer 2002, 43, 6505.
7. Raab, M.; Sčŭdla, J.; Kolařík, J. Eur Polym J 2004, 40, 1317.
8. Menyhárd, A.; Varga, J.; Molnár, G. J Therm Anal Calorim 2006, 83, 625.
9. Feng, J.; Chen, M. Polym Int 2003, 52, 42.
10. Shi, G.; Zhang, X. Thermochim Acta 1992, 205, 235.
11. Mohmeyer, N.; Schmidt, H. W.; Kristiansen, P. M.; Altstädt, V. Macromolecules 2006, 39, 5760.
12. Cao, J.; Zhao, Z. Y.; Du, R. N.; Zhang, Q.; Fu, Q. Plast Rubber Compos 2007, 36, 320.
13. Guo, M. Y.; Yu, L.; Xiong, Z. Q.; Zheng, D.; Wang, W. Z.; Chen, M. C. Polym Mater Sci Eng 2006, 22, 80.
14. Varga, J. J Therm Anal 1989, 35, 1891.
15. Varga, J.; Garzó, G. Angew Makromol Chem 1990, 180, 15.
16. Shi, G. In Progress in Pacific Polymer Science 3; Ghiggino, K. P., Ed.; Springer: Berlin, 1994; Vol. 2, Chapter 20, p 259.
17. Varga, J.; Menyhárd, A. J Therm Anal Calorim 2003, 73, 735.
18. Menyhárd, A.; Varga, J.; Liber, A.; Belina, G. Eur Polym J 2005, 41, 669.
19. Menyhárd, A.; Varga, J. Eur Polym J 2006, 42, 3257.
20. Zhang, R. H.; Shi, D.; Tjong, S. C.; Li, R. K. Y. J Polym Sci Part B: Polym Phys 2007, 45, 2674.
21. Zhang, Z. S.; Tao, Y. J.; Yang, Z. G.; Mai, K. C. Eur Polym J 2008, 44, 1955.
22. Shangguan, Y.; Song, Y.; Peng, M.; Li, B.; Zheng, Q. Eur Polym J 2005, 41, 1766.
23. Li, J. X.; Cheung, W. L.; Jia, D. Polymer 1999, 40, 1219.
24. Li, J. X.; Cheung, W. L. Polymer 1998, 39, 6935.
25. Shen, H.; Wang, Y. H.; Mai, K. C. Thermochim Acta 2007, 457, 27.
26. Somani, R. H.; Hsiao, B. S.; Nogales, A.; Srinivas, S.; Tsou, A. H.; Sics, I.; Balta-Alleja, F. J.; Ezquerra, T. A. Macromolecules 2000, 33, 9385.
27. Somani, R. H.; Hsiao, B. S.; Nogales, A.; Fruitwala, H.; Srinivas, S.; Tsou, A. H.; Somani, R. H.; Hsiao, B. Macromolecules 2001, 34, 5902.
28. Turner Jones, A.; Aizlewood, J. M.; Beckett, D. R. Makromol Chem 1964, 75, 134.
29. Roeder, J.; Oliveira, R. V. B.; Goncalves, M. C.; Soldi, V.; Pires, A. T. N. Polym Test 2002, 21, 815.
30. Tao, Y.; Pan, Y.; Zhang, Z.; Mai, K. Eur Polym J 2008, 44, 1165.
31. Menyhárd, A.; Faludi, G.; Varga, J. J Therm Anal Calorim 2008, 93, 937.
32. Marco, C.; Ellis, G.; Gomez, M. A.; Fatou, J. G.; Arribas, J. M.; Campoy, I.; Fontecha, A. J Appl Polym Sci 1997, 65, 2665.